Structure and Magnetic Properties of Oxygen Pressure Induced $Sr_{1.5}La_{0.5}Cu_{0.5}Ti_{0.5}O_{4-\delta}$ ($0.0 \leq \delta \leq 0.25$)

Song-Ho Byeon* and Haeseung Chung

College of Environment and Applied Chemistry, Institute of Natural Sciences, Kyung Hee University, Kyung Ki 449-701, Korea

Received March 15, 2001. Revised Manuscript Received October 26, 2001

$Sr_{1.5}La_{0.5}Cu_{0.5}Ti_{0.5}O_{4-\delta}$ ($0.0 \leq \delta \leq 0.25$) was investigated to isolate the trivalent state of Cu in an oxygen lattice. $Sr_{1.5}La_{0.5}Cu_{0.5}Ti_{0.5}O_4$, which is free from Cu^{II}, was successfully prepared under 1.5 kbar of oxygen pressure. Structure refinements using X-ray and neutron diffraction patterns provided evidence to support a partial ordering between the Cu and Ti atoms in the *ab*-plane of $Sr_{1.5}La_{0.5}Cu_{0.5}Ti_{0.5}O_{3.75}$ ($\delta = 0.25$). In contrast, no clear evidence for long-range ordering was given in the $Sr_{1.5}La_{0.5}Cu_{0.5}Ti_{0.5}O_{3.82}$ of high Cu^{III} component. The oxygen vacancies were preferentially induced in the in-plane sites rather than the apical sites of the $(Cu,Ti)O_6$ octahedra for all materials of different δ values. The magnetic susceptibilities of materials prepared under N_2 or O_2 flowing condition obeyed a Curie−Weiss law, while the oxygen pressure treated ones showed no constant magnetic moment; a gradual increase of the magnetic moment was observed upon increasing temperature. Moreover, an isotropic signal ($g = 2.13$, $\Delta H = 251$ G) arising from Cu^{III} was observed in ESR spectra of pressure treated materials. On the basis of Rietveld refinements of neutron diffraction data, iodometric titrations, magnetic susceptibility measurements, and pressure dependent ESR studies of $Sr_{1.5}La_{0.5}Cu_{0.5}Ti_{0.5}O_{4-\delta}$, it is proposed that this isotropic signal be attributed to the high-spin state of Cu^{III} ($S = 1$). Such a result is one of the rare examples of high-spin Cu^{III} stabilized in copper-rich oxide.

Introduction

The trivalent state of copper stabilized in an oxide system is of particular interest to the field of high-T_c superconductor because the superconductivity is frequently observed in many oxides with a mixed valence state of copper (Cu^{II}/Cu^{III}). Therefore, the isolation and characterization of Cu^{III} has been an attractive object in solid-state physics and chemistry. Cu^{III}, in an oxygen lattice, can be induced by high oxygen pressure treatment[1,2] or particular electrochemical oxidation at low temperature[3] and chemical oxidation in sodium hypobromite solution.[4] The chemical oxidation procedure has been applied to induce superconductivity by oxygen intercalation into the system $La_{2-x}Sr_xCu_{1-x/2}Ti_{x/2}O_{4-\delta}$, which corresponds to a solid solution between La_2CuO_4 and Sr_2TiO_4.[5] However, this solid solution could not avoid the oxygen vacancy and complete oxidation of copper was not achieved by the chemical oxidation.

In general, the oxygen pressure is useful to stabilize unusually high oxidation states of transition metal ions.[6−9] One example that can be referred to is $Sr_{1.5}La_{0.5}Ni_{0.5}Ti_{0.5}O_4$ with the K_2NiF_4-type structure, which was prepared under high oxygen pressure.[10] The spin-state transition behavior of Co^{III} has been investigated in isostructural $(A,La)_2Co_{0.5}B_{0.5}O_4$ (A = Ca, Sr, Ba; B = Mg, Ti, Zn) lattices which were also prepared under the oxygen pressure.[11,12] Taking into account of these previous results, the oxygen pressure induced $Sr_{1.5}La_{0.5}Cu_{0.5}Ti_{0.5}O_{4-\delta}$ was explored in an attempt to complete the oxidation and isolation of copper. Indeed, $Sr_{1.5}La_{0.5}Cu_{0.5}Ti_{0.5}O_4$, which is free from Cu^{II}, was successfully prepared under 1.5 kbar of oxygen pressure in this work. During ESR study for the characterization of this material, we observed an isotropic signal arising from Cu^{III}. Since trivalent copper is generally stabilized in the low-spin state ($S = 0$) in copper-rich oxide lattices, the observation of such an ESR spectrum was quite interesting. From comparison of powder X-ray and neutron diffraction data, iodometric titration data, magnetic susceptibility data, and pressure dependent

* To whom correspondence should be addressed.

(1) Demazeau, G.; Parent, C.; Pouchard, M.; Hagenmuller, P. *Mater. Res. Bull.* **1972**, *7*, 913.
(2) Goodenough, J. B.; Demazeau, G.; Pouchard, M.; Hagenmuller, P. *J. Solid State Chem.* **1973**, *8*, 325.
(3) Wattiaux, A.; Park, J.-C.; Grenier, J. C.; Pouchard, M. *C. R. Acad. Sci. Ser. 2* **1990**, *310*, 1047.
(4) Schollhorn, R.; Rudolf, P. *J. Chem. Soc., Chem. Commun.* **1992**, 1158.
(5) Steudtner, C.; Moran, E.; Alario-Franco, M.; Martinez, J. L. *J. Mater. Chem.* **1997**, *7*, 661.
(6) Demazeau, G.; Buffat, B.; Menil, F.; Fournes, L.; Pouchard, M.; Dance, J. M.; Fabritchnyi, P.; Hagenmuller, P. *Mater. Res. Bull.* **1981**, *16*, 1465.
(7) Choy, J. H.; Demazeau, G.; Byeon, S.-H. *Solid State Commun.* **1991**, *77*, 647.
(8) Hayashi, K.; Demazeau, G.; Pouchard, M.; Hagenmuller, P. *Mater. Res. Bull.* **1980**, *15*, 461.
(9) Hayashi, K.; Demazeau, G.; Pouchard, M. *C. R. Acad. Sci.* **1981**, *292*, 1433.
(10) Byeon, S.-H.; Demazeau, G.; Choy, J.-H. *Jpn. J. Appl. Phys.* **1995**, *34*, 6156.
(11) Demazeau, G.; Byeon, S.-H.; Hagenmuller, P.; Choy, J.-H. *Z. Anorg. Allg. Chem.* **1992**, *610*, 91.
(12) Demazeau, G.; Byeon, S.-H.; Dance, J. M.; Choy, J.-H.; Pouchard, M.; Hagenmuller, P. *Eur. J. Solid State Inorg. Chem.* **1992**, *29*, 283.

10.1021/cm010221j CCC: $22.00
Published on Web 01/11/2002

ESR spectra of $Sr_{1.5}La_{0.5}Cu_{0.5}Ti_{0.5}O_{4-\delta}$ ($0.0 \leq \delta \leq 0.25$), it is proposed that the isotropic signal observed in the ESR spectrum of $Sr_{1.5}La_{0.5}Cu_{0.5}Ti_{0.5}O_4$ be attributed to the high-spin state ($S = 1$) of Cu^{III}.

Experimental Procedures

$Sr_{1.5}La_{0.5}Cu_{0.5}Ti_{0.5}O_{4-\delta}$ of high oxygen vacancy was prepared by using a solid-state reaction. The stoichiometric mixture of $SrCO_3$, La_2O_3, CuO, and TiO_2 for nominal composition of $Sr_{1.5}La_{0.5}Cu_{0.5}Ti_{0.5}O_4$ was calcined at 950 °C in air for 10 h. The residue was reacted again at 1150 °C in air for 48 h with two intermittent grindings. The reduction and oxidation reactions were carried out by an additional heat treatment at 1150 °C for 10 h under N_2 ($\delta \sim 0.25$) and O_2 ($\delta < 0.25$) flowing conditions, respectively. For further oxidation of the copper ion, the product heated under O_2 gas was subsequently treated at 850 °C under 1.5 kbar of oxygen pressure[13] for 20, 40, and 72 h.

The oxidation numbers of copper and the oxygen vacancies (δ) of materials were determined by typical iodometric titration. The sample powder was dissolved in potassium iodide solution. Liberated iodines were then titrated using sodium thiosulfate solution. All the redox reactions were carried out in an oxygen-free nitrogen gas to avoid the oxidation of iodide ion. The sodium thiosulfate titrant was standardized against potassium iodate and the starch indicator was added just before the end point.

Powder X-ray diffraction patterns were recorded on a rotating anode-installed diffractometer (18 kW). The Cu Kα radiation used was monochromated by a curved-crystal graphite. Neutron powder diffraction measurements were performed on the high-resolution powder diffractometer (HRPD) at the HANARO center of the Korea Atomic Energy Research Institute (KAERI). The structural refinements were achieved using the Rietveld analysis program RIETAN.[14]

The temperature dependence of magnetic susceptibility was measured for the prepared powder samples using SQUID magnetometer in the range of 4−300 K. The thermal variation of molar magnetic susceptibility was corrected from diamagnetic contributions. X-band electron spin resonance (ESR) spectra were obtained by using Bruker ER 200 tt spectrometer. The applied magnetic field was standardized by NMR gaussmeter using the resonance of proton. Hewlett-Packard 5342 A was used for the measurement of the frequency.

Results and Discussion

Qualitative Analyses and X-ray Diffractions. The quantity of materials recovered after oxygen pressure treatment were less than 80 mg. To obtain X-ray powder diffraction data of pressure treated products, a small amount of powder material was dispersed on a glass plate with absolute ethanol. Lattice parameters were derived from least-squares refinement of the diffraction data. X-ray powder diffraction patterns of selected samples are compared as a function of their synthetic condition as shown in Figure 1. All the materials prepared in this work are characterized by typical K_2NiF_4-type structure. No evident additional diffraction peaks resulting from a long-range ordering between the Cu and Ti atoms are observed. Consequently, their reflections could be indexed on a tetragonal symmetry with the unit cell parameters $a \sim 3.8$ Å and $c \sim 12.7$ Å. A slight amount of impurity phase, whose related diffraction peaks are indicated by arrows, corresponds to Sr_2CuO_3.[15] As can be seen in Figure 1, this impurity decreases when the material was oxidized in O_2 gas and ultimately disappears after the treatment under oxygen pressure.

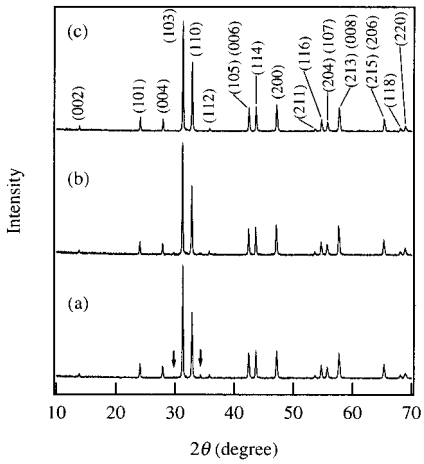

Figure 1. Powder X-ray diffraction patterns of $Sr_{1.5}La_{0.5}Cu_{0.5}Ti_{0.5}O_{4-\delta}$ prepared under (a) N_2 gas, (b) O_2 gas, and (c) 1.5 kbar of oxygen pressure. All reflections are indexed on the basis of *I*4/*mmm* space group. The additional reflections indicated by arrows are related to the Sr_2CuO_3 impurity phase.

The relationship of preparation conditions, compositions, and unit cell parameters is summarized in Table 1. This table shows that a complete oxidation of copper can be achieved by treatment under oxygen pressure for sufficient time. Lower oxygen vacancy gives rise to a slight lattice contraction. In particular, an increase of Cu^{III} content (i.e. decrease of the oxygen vacancy) leads to a decrease in the *c* parameter. Such a behavior would result from a reduced Jahn−Teller effect because of decreased Cu^{II} (d^9) content by oxidation. Compared with those of $La_2Cu_{0.5}Li_{0.5}O_4$ ($c/a \sim 3.54$)[1] and even metallic $SrLaCuO_4$ ($c/a \sim 3.53$),[2] which are free from Cu^{II}, the c/a ratios of $Sr_{1.5}La_{0.5}Cu_{0.5}Ti_{0.5}O_{4-\delta}$ are significantly small (~ 3.31). This indicates that strongly covalent Ti − O bonds competing with Cu − O ones in the *ab*-plane of the lattice largely reduce the tetragonal elongation of CuO_6 octahedra along the *c* axis.

Neutron Diffractions. To determine the structural type, particularly an arrangement mode of the Cu and Ti atoms in the *ab*-plane and a degree of tetragonal distortion of CuO_6 octahedra, the neutron diffraction study was performed. Because of too small an amount of pressure treated materials, the neutron diffraction patterns could be measured only for the materials before oxygen pressure treatment, $Sr_{1.5}La_{0.5}Cu_{0.5}Ti_{0.5}O_{3.75}$ and $Sr_{1.5}La_{0.5}Cu_{0.5}Ti_{0.5}O_{3.82}$. On the basis of X-ray diffraction patterns, the most probable space group of $Sr_{1.5}La_{0.5}Cu_{0.5}Ti_{0.5}O_{4-\delta}$ system is expected to be *I*4/*mmm*. The Cu and Ti atoms are randomly arranged in the *ab*-plane with this structure. Indeed, adoption of the space group *I*4/*mmm* gave an excellent fit to the neutron diffraction

(13) Demazeau, G. Thesis, Universite de Bordeaux I, 1973.
(14) Izumi, F.; Murata, H.; Watanabe, N. *J. Appl. Crystallogr.* **1987**, *20*, 411.
(15) Teske, C.; Muller-Buschbaum, H. *Z. Anorg. Allg. Chem.* **1969**, *371*, 325.

Table 1. Comparison of Preparation Conditions, Compositions, and Unit Cell Parameters of $Sr_{1.5}La_{0.5}Cu_{0.5}Ti_{0.5}O_{4-\delta}$ and Some Reference Compounds with Similar Structure

condition	composition	unit cell parameter		*c*/*a* ratio
		a (Å)	*c* (Å)	
N_2 flow	$Sr_{1.5}La_{0.5}Cu_{0.5}Ti_{0.5}O_{3.75(2)}$ [b]	3.8517(1)[a, c]	12.7693(5)[a, c]	3.31
O_2 flow	$Sr_{1.5}La_{0.5}Cu_{0.5}Ti_{0.5}O_{3.82(3)}$ [b]	3.8510(1) [c]	12.7591(5) [c]	3.31
PO_2 =1.5 kbar, 20 h	$Sr_{1.5}La_{0.5}Cu_{0.5}Ti_{0.5}O_{3.90(2)}$ [b]	3.848(1) [d]	12.75(1) [d]	3.31
PO_2 =1.5 kbar, 40 h	$Sr_{1.5}La_{0.5}Cu_{0.5}Ti_{0.5}O_{3.97(1)}$ [b]	3.846(1) [d]	12.74(1) [d]	3.31
PO_2 =1.5 kbar, 72 h	$Sr_{1.5}La_{0.5}Cu_{0.5}Ti_{0.5}O_{4.00(1)}$ [b]	3.847(1) [d]	12.74(1) [d]	3.31
PO_2 =1.6 kbar, 48 h	$La_2Cu_{0.5}Li_{0.5}O_4$ [e]	3.731	13.20	3.54
PO_2 =3 kbar, 42 h	$SrLaCuO_4$ [f]	3.765	13.27	3.53

[a] A partial ordering between the Cu and Ti atoms was ignored for comparison. If the super-structure is considered, the unit cell parameters are refined to $a = 5.4470(2)$ Å and $c = 12.7693(5)$ Å. See the text. [b] The oxygen content was determined by the iodometric titration. [c] Unit cell parameters were determined by the neutron diffraction. [d] Unit cell parameters were determined by the X-ray diffraction. [e] Reference (1). [f] Reference (2).

data of $Sr_{1.5}La_{0.5}Cu_{0.5}Ti_{0.5}O_{3.75}$ (a = 3.8517(1) Å, c = 12.7693(5) Å, R_{WP} = 6.12%, R_I = 2.88%). Several reflections related to the Sr_2CuO_3 impurity phase were ignored during refinement. Calculated lengths of the in-plane (Cu,Ti) − O average bond (1.9258 Å) and the apical (Cu,Ti) − O one (2.083 Å) were quite different from those of La_2CuO_4 and $SrLaCuO_4$, which contain only Cu^{II} and Cu^{III}, respectively. The in-plane Cu − O bond lengths are 1.90 Å and 1.88 Å and the apical ones are 2.40 Å and 2.33 Å for La_2CuO_4 and $SrLaCuO_4$, respectively.[2,16] Hence, it could be deduced that, compared with those in typical K_2NiF_4-type cuprates, a tetragonal elongation of CuO_6 octahedron would be very weak in $Sr_{1.5}La_{0.5}Cu_{0.5}Ti_{0.5}O_{3.75}$.

All of above crystallographic data based on the *I*4/*mmm* space group seem to indicate that there is no long-range ordering between the Cu and Ti atoms in the *ab*-plane. However, several additional weak reflections were observed after the profile for $Sr_{1.5}La_{0.5}Cu_{0.5}Ti_{0.5}O_{3.75}$ was refined on the basis of such a body-centered cell. The most interesting feature was the observation of reflections which are not indexed under the extinction condition, $h + k + l = 2n$ for *hkl* reflections. Frequently the 1:1 ordering between two cations occurs in the K_2NiF_4-type lattices when there is a sufficient difference in ionic radius and/or charge of cations in the *ab*-plane. Many evidences for the superlattice resulting from the long-range ordering of (Li^I, Mn^{IV}), (Li^I, Fe^{IV}), (Li^I, Co^{III}), (Li^I, Ni^{III}), (Mg^{II}, Fe^{IV}), (Mg^{II}, Co^{III}), (Mg^{II}, Ni^{III}), (Zn^{II}, Fe^{IV}), (Zn^{II}, Co^{III}), and (Zn^{II}, Ni^{III}) cationic pairs in the *ab*-plane of the K_2NiF_4-type structure have been observed in corresponding Guinier films, Mössbauer spectra, and electron diffraction photographs.[11,12,17−20] The crystal structure is then characterized by the space group *P*422. Figure 2 shows the relationship between the space group *I*4/*mmm* (a_0, c_0) and *P*422 ($a \sim a_0\sqrt{2}$, $c \sim c_0$). Even in the superlattice induced by an intra-plane ordering, there is no inter-plane ordering along the direction [101]. Thus, both Cu and Ti can exist at the (0.5,0,0.5) position as a neighboring atom of Cu at the (0,0,0) position.

Taking into account these structural features, the refinement of neutron diffraction data for $Sr_{1.5}La_{0.5}Cu_{0.5}Ti_{0.5}O_{3.75}$ was carried out again with the space group *P*422. As shown in Figure 3, the additional weak reflections which are not indexed on the basis of the *I*4/*mmm* space group are assigned to (103), (211), (302),

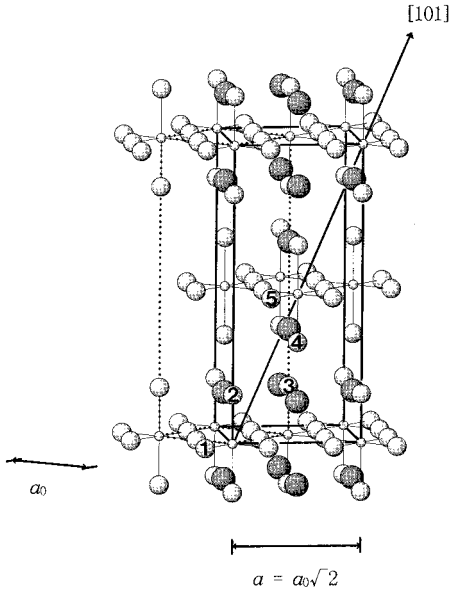

Figure 2. Idealized structure of $Sr_{1.5}La_{0.5}Cu_{0.5}Ti_{0.5}O_4$. A disordered structure of *I*4/*mmm* space group is described by dotted lines (a_0 and c_0). The long-range ordering between the Cu and Ti atoms in the intra-plane results in a superstructure (bold lines) of unit cell parameters, $a \sim a_0\sqrt{2}$ and $c \sim c_0$. The space group *P*422 is then adopted to an ordered structure. However, there is no inter-plane ordering along the [101] axis represented by arrow. Cu and Ti = small black and white spheres, La = large shaded spheres, O = large white spheres.

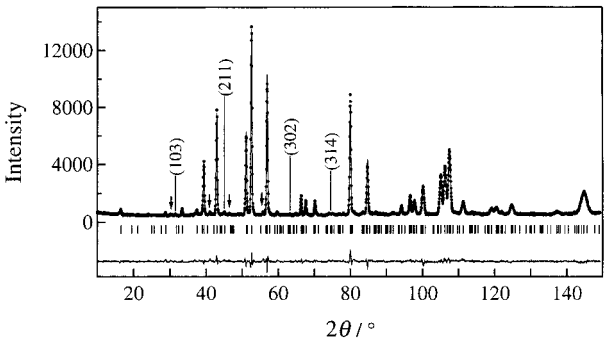

Figure 3. Calculated (solid line), experimental (dotted line), and difference (solid lines on the bottom) for the neutron powder diffraction pattern of $Sr_{1.5}La_{0.5}Cu_{0.5}Ti_{0.5}O_{3.75}$ with the space group *P*422. The reflections marked with arrows are related to the impurity phase, Sr_2CuO_3.

(16) Longo, J. M.; Raccah, P. M. *J. Solid State Chem.* **1973**, *6*, 526.
(17) Demazeau, G.; Marty, J. L.; Pouchard, M.; Rojo, T.; Dance, J. M.; Hagenmuller, P. *Mater. Res. Bull.* **1981**, *16*, 47.
(18) Mohan Ram, R. A.; Singh, K. K.; Madhusudan, W. H.; Ganguly, P.; Rao, C. N. R. *Mater. Res. Bull.* **1983**, *18*, 703.
(19) Demazeau, G.; Zhu, L. M.; Fournes, L.; Pouchard, M.; Hagenmuller, P. *J. Solid State Chem.* **1988**, *72*, 31.
(20) Byeon, S.-H.; Demazeau, Z.; Choy, J.-H.; Hagenmuller, P. *C. R. Acad. Sci.* **1991**, *312*, 37.

Table 2. Neutron Powder Diffraction Data[a] of $Sr_{1.5}La_{0.5}Cu_{0.5}Ti_{0.5}O_{3.75}$ with the Space Group *P*422[c]

a (Å)				5.4470(2)		
c (Å)				12.7693(5)		
V (Å^3)				378.86(2)		
Bragg (R_I, %)				2.79		
weighted profile (R_{WP}, %)				5.91		
profile (R_P, %)				4.61		
expected (R_E, %)				3.39		
	atom	g^b	x	y	z	B(Å^2)
atomic positions and isotropic temperature factors	Sr,La1	1.0	0.5	0.0	0.1462(4)	0.9(1)
	Sr,La2	1.0	0.0	0.0	0.3606(4)	0.3(2)
	Sr,La3	1.0	0.5	0.5	0.3540(8)	0.5(2)
	Cu1	0.83(4)	0.0	0.0	0.0	1.5(5)
	Ti1	0.17(4)	0.0	0.0	0.0	1.6(7)
	Cu2	0.17(4)	0.5	0.5	0.0	1.7(9)
	Ti2	0.83(4)	0.5	0.5	0.0	1.8(6)
	Cu,Ti3	1.0	0.5	0.0	0.5	1.8(4)
	O1	0.87(4)	0.240(2)	0.240(2)	0.0	1.4(3)
	O2	1.01(1)	0.0	0.0	0.162(1)	2.9(4)
	O3	0.96(4)	0.5	0.5	0.163(1)	0.8(4)
	O4	1.00(1)	0.5	0.0	0.336(1)	2.0(3)
	O5	0.93(3)	0.254(1)	0.254(1)	0.5	0.4(3)

[a] Wavelength of neutron = 1.8346 Å. [b] Site occupancy. [c] Linear constrains; g(Ti1) = 1 − g(Cu1), g(Cu2) = 1 − g(Cu1), g(Ti2) = g(Cu1).

and (314) reflections with the *P*422 space group. Some crystallographic data, final reliability factors, refined atomic positions, and isotropic thermal factors are listed in Table 2. Although the thermal factors of the Cu and Ti atoms are relatively large because of several linear constrains, the site occupancies of Cu1 (0.83) and Cu2 (0.17) suggest a partial ordering of ∼ 34% in the *ab*-plane. Total amount of oxygen (∼ 3.78) per unit formula, which was obtained by structural refinement, is in agreement with that (3.75(2)) determined by chemical titration. A lower number of site occupancies exist for the O1 and O5 sites than for the O2 and O4 sites, implying that the predominant oxygen vacancies are located at the in-plane oxygen sites rather than the apical oxygen sites. Compared with those of the in-plane oxygen atoms (O1 and O5), the thermal factors of the apical oxygen atoms (O2 and O4) are relatively large because these atoms are weakly bonded to Cu or Ti. This is a typical behavior for the K_2NiF_4-type oxide lattice. It is interesting that the thermal factor of O3 is much smaller than those of other apical oxygens, O2 and O4. Since the O3 atom is on the apical position of the (Cu2,Ti2)O_6 octahedron containing only 0.17 of Cu2, the low thermal factor of O3 can be attributed to a reduced tetragonal elongation of the Cu^{II}-poor octahedral site. The bond lengths calculated on the basis of the *P*422 space group are summarized in Table 3. It should be noted that the length of a (Cu,Ti) − O average bond is significantly different depending on the Cu content in the octahedral site. If we compare the bond lengths of (Cu1,Ti1)O_6, (Cu2,Ti2)O_6, and (Cu3,Ti3)O_6 octahedra, a difference between the apical and in-plane bond length is the smallest for Cu-poor (Cu2,Ti2)O_6 octahedron. A degree of octahedral distortion could be represented by the bond length ratio (θ = d{in-plane (Cu,Ti) − O}/d{axial (Cu,Ti) − O}), which increases from 0.898 for Cu-rich (Cu1,Ti1)O_6 octahedron to 0.920 and 0.966 for average (Cu3,Ti3)O_6 and Cu-poor (Cu2,Ti2)O_6 octahedron, respectively. The lowest elongation of (Cu2,Ti2)O_6 octahedron is well correlated to the weakest Jahn−Teller effect in Cu^{II} (d^9)-poor site.

Despite slightly improved reliability factors, when the *P*422 space group rather than the *I*4/*mmm* one was adopted for $Sr_{1.5}La_{0.5}Cu_{0.5}Ti_{0.5}O_{3.75}$, the difference in the profile fit of the neutron diffraction pattern was relatively small because of only a partial ordering (∼ 34%) between the Cu and Ti atoms. If we consider the lattice energy, an additional Madelung energy resulting from cationic ordering in a typical perovskite lattice is much higher than that in the K_2NiF_4-type lattice.[21−23] Nevertheless, the (Cu^{II}, Ti^{IV}) pair is not completely ordered in $LaCu_{0.5}Ti_{0.5}O_3$ perovskite lattice.[24] Consequently, the amount of additional lattice energy should be insufficient for a complete long-range ordering of such cations in the K_2NiF_4-type lattice.

Table 3. Selected Bond Lengths of $Sr_{1.5}La_{0.5}Cu_{0.5}Ti_{0.5}O_{3.75}$ Obtained with Space Group *P*422

bond	length (Å)
Sr,La1−O1 (x 4)	2.684(4)
Sr,La1−O2 (x 2)	2.731(1)
Sr,La1−O3 (x 2)	2.732(1)
Sr,La1−O4 (x 1)	2.42(1)
Sr,La2−O2 (x 1)	2.54(2)
Sr,La2−O4 (x 4)	2.741(1)
Sr,La2−O5 (x 4)	2.644(8)
Sr,La3−O3 (x 1)	2.44(2)
Sr,La3−O4 (x 4)	2.733(1)
Sr,La3−O5 (x 4)	2.660(9)
Cu1,Ti1−O1 (x 4)	1.85(1)
Cu1,Ti1−O2 (x 2)	2.06(2)
Cu2,Ti2−O1 (x 4)	2.01(1)
Cu2,Ti2−O3 (x 2)	2.08(1)
Cu3,Ti3−O4 (x 2)	2.094(9)
Cu3,Ti3−O5 (x 4)	1.9260(1)

On the other hand, no clear extra diffractions resulting from such a long-range ordering between Cu and Ti were detected in the neutron diffraction pattern of $Sr_{1.5}La_{0.5}Cu_{0.5}Ti_{0.5}O_{3.82}$. A poor fit with large reliability factors and negative isotropic thermal parameters for the oxygen atoms was obtained when the space group *P*422 was tested for this material. In contrast, adoption of the space group *I*4/*mmm* gave an excellent fit to the neutron diffraction data. This suggested that there is no partial ordering between the Cu and Ti atoms in the *ab*-plane of $Sr_{1.5}La_{0.5}Cu_{0.5}Ti_{0.5}O_{3.82}$. A calculation using the oxygen content of 3.82 gives the formal oxidation state of +2.28 for the Cu ion. Compared with that (Δ = 2) in the Cu^{III}-free system, a decrease of charge difference (Δ = 1.72) could be one of important factors inducing a random arrangement of the Cu and Ti ions in the mixed valence system. The ionic size difference must also be considered. If we compare the radii of Cu^{II} (r = 0.73 Å), Cu^{III} (r = 0.54 Å), and Ti^{IV} (r = 0.605 Å),[25] there is a much smaller size difference (0.065 Å) between Cu^{III} and Ti^{IV} than (0.125 Å) between Cu^{II} and Ti^{IV}. This is coupled with a smaller charge difference and will not be sufficient to induce a partial ordering in the *ab*-plane. The observed, calculated, and difference profile fit for $Sr_{1.5}La_{0.5}Cu_{0.5}Ti_{0.5}O_{3.82}$ is shown in Figure 4. The diffraction intensities attributed to the Sr_2CuO_3 impurity phase are significantly reduced and not clearly detectable. The final reliability factors, refined atomic positions, and isotropic thermal factors are listed in Table 4. The total amount of oxygen (∼ 3.81) per unit formula obtained by structural refinement is practically

(21) Byeon, S.-H.; Kim, I. S.; Itoh, M.; Nakamura, T. *Mater. Res. Bull.* **1993**, *28*, 597.
(22) Rosenstein, R. D.; Schor, R. *J. Chem. Phys.* **1963**, *38*, 1789.
(23) Rosenstein, R. D.; Schor, R. *J. Chem. Phys.* **1965**, *42*, 3698.
(24) Ramadass, N.; Gopalakrishnan, J.; Sastri, M. V. *J. Inorg. Nucl. Chem.* **1978**, *40*, 1453.
(25) Shannon, R. D. *Acta Crystallogr. A* **1976**, *32*, 751.

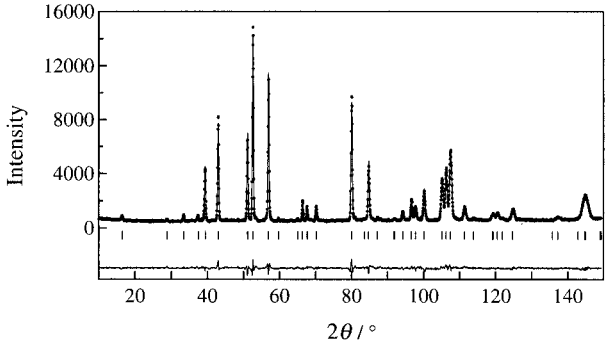

Figure 4. Calculated (solid line), experimental (dotted line), and difference (solid lines on the bottom) for the neutron powder diffraction pattern of $Sr_{1.5}La_{0.5}Cu_{0.5}Ti_{0.5}O_{3.82}$ with the space group *I*4/*mmm*.

Table 4. Neutron Powder Diffraction Data[a] of $Sr_{1.5}La_{0.5}Cu_{0.5}Ti_{0.5}O_{3.82}$ with the Space Group *I*4/*mmm*

a (Å)	3.8510(1)
c (Å)	12.7591(4)
V (Å^3)	189.22(1)
Bragg (R_I, %)	2.71
weighted profile (R_{WP}, %)	6.19
profile (R_P, %)	4.82
expected (R_E, %)	3.32

	atom	g^b	*x*	*y*	*z*	*B*(Å^2)
atomic positions	Sr,La	1.0	0.0	0.0	0.3561(1)	0.59(4)
and isotropic	Cu,Ti	1.0	0.0	0.0	0.0	1.8(1)
temperature	O1	0.905(6)	0.0	0.5	0.0	1.02(4)
factors	O2	1.004(9)	0.0	0.0	0.1632(1)	1.85(6)

[a] Wavelength of neutron = 1.8346 Å. [b] Site occupancy.

Table 5. Selected Bond Lengths of $Sr_{1.5}La_{0.5}Cu_{0.5}Ti_{0.5}O_{3.82}$ Obtained with Space Group *I*4/*mmm*

bond	length (Å)
Sr,La−O1 (x 4)	2.661(1)
Sr,La−O2 (x 4)	2.7342(2)
Sr,La−O2 (x 1)	2.461(2)
Cu,Ti−O1 (x 4)	1.9255(1)
Cu,Ti−O2 (x 2)	2.082(2)

the same as that (3.82(3)) determined by chemical titration. Lower occupancy observed for the O1 sites than for the O2 sites confirms that higher oxygen vacancy of the in-plane oxygen sites rather than the apical ones are retained for all solid-solution ranges. Selected bond lengths of $Sr_{1.5}La_{0.5}Cu_{0.5}Ti_{0.5}O_{3.82}$ are summarized in Table 5. Based on the lengths of the in-plane (Cu,Ti) − O average bond (1.9255 Å) and apical (Cu,Ti) − O one (2.082 Å), the distortion degree (θ = 0.925) of the (Cu,Ti)O_6 octahedron in $Sr_{1.5}La_{0.5}Cu_{0.5}Ti_{0.5}O_{3.82}$ is lower than that (θ = 0.920) of the (Cu3,Ti3)O_6 octahedron, half of which is occupied by Cu3 in $Sr_{1.5}La_{0.5}Cu_{0.5}Ti_{0.5}O_{3.75}$ (see Table 3). This result indicates that an elongation of the (Cu,Ti)O_6 octahedron is reduced upon decreasing the amount of Jahn−Teller ion (Cu^{II}) by oxidation. Although the neutron diffraction study was limited to the materials before oxygen pressure treatment because of too small an amount of pressure treated materials, it could be deduced that the tetragonal elongation of CuO_6 octahedron will be gradually reduced when this material is further oxidized by high oxygen pressure.

Magnetic Susceptibilities. Figure 5 shows the inverse magnetic susceptibility data of $Sr_{1.5}La_{0.5}Cu_{0.5}Ti_{0.5}O_{4-\delta}$ as a function of temperature. The magnetic property of $Sr_{1.5}La_{0.5}Cu_{0.5}Ti_{0.5}O_{3.75}$ prepared under N_2 flowing condition obeys a Curie−Weiss law and the observed effective magnetic moment of ~ 1.73 μ_B/Cu is in good agreement with the theoretical spin-only value of 1.73 μ_B for Cu^{II}. The magnetic behavior of $Sr_{1.5}La_{0.5}Cu_{0.5}Ti_{0.5}O_{3.82}$ prepared under an O_2 flowing condition also obeys a Curie−Weiss law, but the effective magnetic moment of ~ 1.43 μ_B/Cu is much lower than the theoretical spin-only one for Cu^{II}. If we suppose that Cu^{III} (d^8) is in a diamagnetic low-spin configuration in this material, such an effective magnetic moment is attributed to ~ 3.81 of oxygen content per formula unit, supporting the result of 3.82 from chemical titration. This indicates that the magnetic behaviors of these oxides are dominated by the presence of Cu^{II}. On the contrary, the oxygen pressure treated samples show no constant magnetic moment in the measured temperature range as shown in Figures 5c and 5d. This magnetic behavior was reproducible even after three cycles of a cooling and heating process. Moreover, the effective magnetic moment of $Sr_{1.5}La_{0.5}Cu_{0.5}Ti_{0.5}O_{4.00}$, which is free from Cu^{II}, is close to ~ 1.2 μ_B/Cu at approximately room temperature. Referring to the result from chemical titration, such a magnetic moment cannot be ascribed to the Cu^{II} impurity. One possible explanation could be proposed by supposing that the low-spin (S = 0) and high-spin states (S = 1) of the Cu^{III} ions are in equilibrium in oxygen pressure induced phases. A shift of equilibrium to the high-spin state would account for a gradual increase of magnetic moment with increasing temperature. If we compare the theoretical one (2.83 μ_B) for the high-spin Cu^{III}, the magnetic moment (~ 1.2 μ_B/Cu) measured for $Sr_{1.5}La_{0.5}Cu_{0.5}Ti_{0.5}O_{4.00}$ near room temperature could result from ~ 42% of the copper ion stabilized in the high-spin state at approximately room temperature. Considering that the trivalent copper ion is known to generally adopt a low-spin configuration in oxide lattices,[1,26] such a magnetic behavior related to trivalent copper ion was surprising. Accordingly, the ESR spectra of prepared materials were examined to confirm the origin of this magnetic moment.

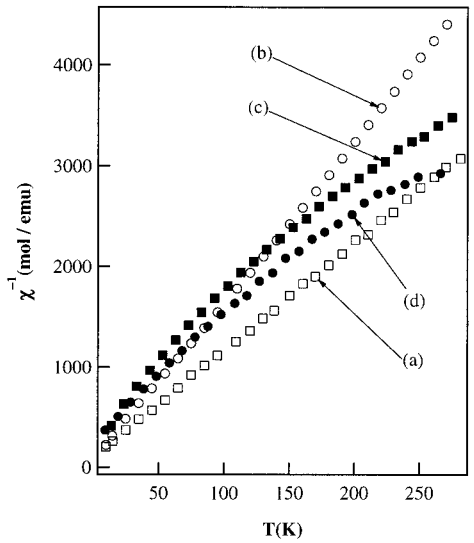

Figure 5. Inverse magnetic susceptibility as a function of temperature for $Sr_{1.5}La_{0.5}Cu_{0.5}Ti_{0.5}O_{4-\delta}$ prepared under N_2 flow (a), O_2 flow (b), and after treatment at 850 °C under 1.5 kbar of oxygen pressure for 20 h (c) and 72 h (d).

(26) Ovshinsky, S. R.; Hudgens, S. J.; Lintveldt, R. L.; Rorabacher, D. B. *Mod. Phys. Lett.* **1987**, *B1*, 275.

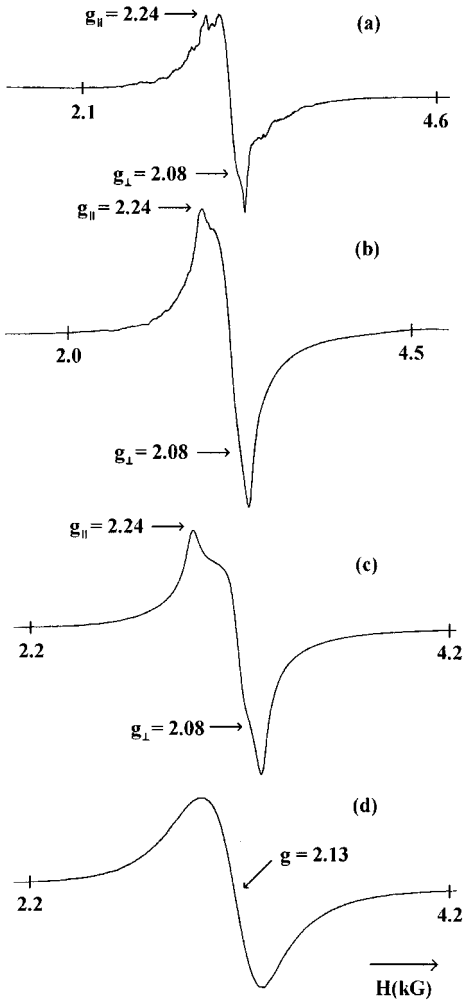

Figure 6. X-band ESR spectra of $Sr_{1.5}La_{0.5}Cu_{0.5}Ti_{0.5}O_{4-\delta}$ before (a) and after treatment at 850 °C under 1.5 kbar of oxygen pressure for 20 h (b), 40 h (c), and 72 h (d).

Electron Spin Resonance Spectra. The ESR spectrum (Figure 6a) for $Sr_{1.5}La_{0.5}Cu_{0.5}Ti_{0.5}O_{3.82}$ exhibits a pronounced signal at $g_\perp = 2.08$ and a poorly resolved one at $g_\parallel = 2.24$. The poor signal arises from parallel hyperfine splitting. Such a spectral feature is characteristic of the Cu^{II} (d^9) ion in axially distorted octahedral site.[27] After further oxidation of this material under oxygen pressure, the hyperfine structure of the anisotropic signal gradually disappears while a relatively broad isotropic signal appears with increasing the oxygen content (Figures 6b and 6c). Ultimately, only isotropic signal centered on $g = 2.13$ ($\Delta H = 251$ G) is observed in the $Sr_{1.5}La_{0.5}Cu_{0.5}Ti_{0.5}O_4$ which is free from the Cu^{II} component (Figure 6d).

Taking into account the results of chemical titration and magnetic susceptibility measurement, the anisotropic line clearly arises from the Cu^{II} component in $Sr_{1.5}La_{0.5}Cu_{0.5}Ti_{0.5}O_{4-\delta}$. On the other hand, broad isotropic signal observed with $Sr_{1.5}La_{0.5}Cu_{0.5}Ti_{0.5}O_4$ containing no Cu^{II} component is most likely ascribed to the high-spin Cu^{III} ($S = 1$). The ground term of d^8 configuration is strongly dependent on the site distortion.[28] A strong distortion considerably stabilizes the $S = 0$ term, but a weak distortion is preferable to the $S = 1$ term. When the Cu^{III} ion is surrounded by four weak Li − O bonds competing with Cu − O bonds as in $La_2Li_{0.5}Cu_{0.5}O_4$,[1] the low-spin state of Cu^{III} is consequently stabilized in a highly elongated octahedral site because of the strong crystal field in the *ab*-plane. In contrast, the CuO_6 octahedra of $Sr_{1.5}La_{0.5}Cu_{0.5}Ti_{0.5}O_{4-\delta}$ system would be applied by a weak and almost cubic crystal field when they are surrounded by four strong Ti − O bonds competing with Cu − O bonds in the *ab*-plane. A random arrangement of Cu^{III} and Ti^{IV} will make such an octahedra with the probability of 25%. Moreover, the degree of tetragonal elongation of a $(Cu,Ti)O_6$ octahedra is lowered with increasing Cu^{III} content as evidenced in the neutron diffraction data. Weak tetragonal elongation of a CuO_6 octahedra would give rise to only a weak energy separation between d_{z2} − and d_{x2-y2} − orbitals of copper in $Sr_{1.5}La_{0.5}Cu_{0.5}Ti_{0.5}O_4$. The ground state, ^3F, of high-spin Cu^{III} is then split by the psudocubic field into an $^3A_2$ singlet and two upper $^3T_2$ and $^3T_1$ triplets. The ground state and the excited states will be mixed by the contribution of spin−orbit coupling and the presence of a weak distortion.[29] Because our spectra were recorded on the powdered copper-rich samples, it can be expected that the zero-field splitting will contribute only to the line broadening.

In fluorides, the high-spin state of Cu^{III} is frequently observed. Examples of these types of fluorides are Cs_2KCuF_6, Na_3CuF_6, and K_2NaCuF_6. The effective magnetic moment of 2.77 μ_B obtained from the magnetic susceptibility data of copper-rich fluoride, Na_3CuF_6, was close to the theoretical spin-only magnetic moment 2.83 μ_B for the high-spin Cu^{III}.[30] Subsequently, an isotropic ESR signal centered on $g = \sim 2.12$ was also observed in Na_3CuF_6 and K_2NaCuF_6.[31] In contrast to the fluoride system, the high-spin Cu^{III} is rarely observed in Cu-rich oxide lattices. Only a few examples have been characterized by ESR particularly in Cu-doped oxides. For instance, a quasi isotropic line centered on $g = 2.077$ and a zero-field splitting $D = -0.1884$ cm^{-1} resulting from the trigonal distortion of AlO_6 octahedra was observed in ESR spectra of Cu-doped Al_2O_3 single crystal.[32,33] Our result is one of the rare examples of the high-spin Cu^{III} stabilized in a copper-rich oxide system.

Acknowledgment. We are grateful to the Ministry of Science and Technology for providing the program to use of Neutron diffraction facilities at the HANARO. This work was supported by grant No. R01-2001-00045 from the KOSEF.

CM010221J

(27) Al'tshuler, S. A.; Kozyrev, B. M. *Electron Paramagnetic Resonance in Compounds of Transition Elements*; John Wiley & Sons: New York, 1974; p 358 and references therein.

(28) Buffat, B.; Demazeau, G.; Pouchard, M.; Hagenmuller, P. *Proc. Indian Acad. Sci.* **1984**, *93*, 313.

(29) Wertz, J. E.; Bolton, J. R. *Electron Spin Resonance, Elementary Theory and Applications*, McGraw-Hill: New York, 1972; p 292.

(30) Grannec, J.; Portier, J.; Pouchard, M.; Hagenmuller, P. *J. Inorg. Nucl. Chem.* **1976**, 119.

(31) Dance, J. M.; Grannec, J.; Tressaud, A. *Eur. J. Solid State Inorg. Chem.* **1988**, *25*, 621.

(32) Blumberg, W. E.; Eisinger, J.; Geschwind, S. *Phys. Rev.* **1963**, *130*, 900.

(33) Kamimura, H. *Phys. Rev.* **1962**, *128*, 1077.